Final Report

Federal Agency and Organization Element to Which Report is Submitted	Department of Energy – National Energy Technology Laboratory (NETL)
Federal Grant Number	**DE-EE0008857**
Project Title	**Hot Pressing of Reinforced Li-NMC All-Solid State Batteries with Sulfide Glass Electrolyte**
Principal Investigator Name, Title, Contact Information	Thomas Yersak Senior Researcher General Motors LLC GM Global Research and Development 30500 Mound Road Warren, Michigan 48092-2031 Tel: (586) 596-4392 Email: thomas.yersak@gm.com
Submitting Official Name, Title, Contact Information	Aida Rodrigues Manager – Government Contracts General Motors LLC 850 North Glenwood Avenue Pontiac, MI 48340-2920 Tel: (585) 303-6601 Email: aida.rodrigues@gm.com
Submission Date	09/30/2023
DUNS Number	076336064
Recipient Organization (associated with DUNS Number)	General Motors LLC 850 North Glenwood Avenue Pontiac, MI 48340-2920
Project /Grant Period	10/01/2019 to 06/30/2023
Reporting Period End Date	06/30/2023
Report Term or Frequency	Final Report

Advanced Materials R&D

Beyond Li-ion R&D: Solid-State Batteries

Final Report: Hot Pressing of Reinforced All-solid-state Batteries with Sulfide Glass Electrolyte (General Motors LLC)

Thomas A. Yersak, Principal Investigator
General Motors LLC
GM Global Research and Development
30470 Harley Earl Blvd.
Warren, Michigan 48092-2031
E-mail: thomas.yersak@gm.com

Tien Duong, DOE [Program/Technology Development] Manager
U.S. Department of Energy
E-mail: tien.duong@ee.doe.gov

Start Date: October 1, 2019 End Date: June 30, 2023

Project Introduction

The performance of solid-state batteries (SSBs) with sulfide solid-state electrolytes (SSEs) is limited because they are 10 - 30% porous. Porosity limits energy density of the composite cathode and provides a conduit for Li-metal deposits through the separator if operating specifications (*e.g.* current density, operating temperature, and pressure) are not strictly conrolled. This project intends to demonstrate that hot press cell processing and appropriately formulated sulfide glass SSEs can eliminate porosity to enable SSBs with energy density of $\geq$ 350 Wh/kg.

Objectives

The objective of this project is to research, develop, and test SSBs capable of achieving program performance metrics by implementing appropriately formulated sulfide glass SSEs and hot press cell processing in a dry room environment. In the composite cathode, hot pressing eliminates porosity to increase energy density by enabling thick composite cathodes with high active material loading. In the separator, hot pressing eliminates porosity that may otherwise provide a conduit for Li metal deposits to short the cell.

Outline

This project's final report will be divided into three sections. In the first section, a Li/S semi-solid cell design will be described that shows program performance metrics can be met [1]. The technical achievements enabling this cell design will then be described; namely, fabrication of a reinforced LiPSiS glass SSE separator by hot pressing [1] and chemical compatibility between LiPSiS glass SSE and DME:DOL based liquid electrolyte [2]. In the second section, we will outline several opportunities for how the aforementioned cell design can be improved. In the third and final section, we then go on to describe progress towards an improved cell design including evaluation of sulfide SSE moisture stability in a dry room environment [3], development of a highly processable oxysulfide glass SSE composition, development of hot-pressed all-solid-state cathode composites [4], and development of a semi-solid electrolyte system comprising oxysulfide SSE and solvate ionic liquid (SIL) electrolyte.

Results

I. Cell Design

The performance of Li/S battery cells can be improved by integrating solid-state electrolytes (SSEs) into the cell design. In Li/S cells with highly solvating electrolytes, a major problem is the migration of dissolved polysulfide species to the anode [5], which results in a parasitic polysulfide shuttle that reduces cell coulombic efficiency. A $LiNO_3$ co-salt may be used to inhibit the polysulfide redox shuttle, however, its continual consumption generates gas and increases cell impedance over time [6, 7]. Impermeable SSE separators have been used to physically block the migration of polysulfide and eliminate the need for $LiNO_3$ co-salt. Previous reports utilize thick oxide ceramic SSE pellets composed of $Li_{1.3}Al_{0.3}Ti_{1.7}(PO_4)_3$ (LATP) [8-10], $Li_{1+x}Y_xZr_{2-x}(PO_4)_3$ (LYZP) [11], $Li_{1.5}Al_{0.5}Ge_{1.5}(PO_4)_3$ (LAGP) [12], and $Li_7La_3Zr_2O_{12}$ (LLZO) [13]. Unfortunately, these aforementioned oxide SSE separators greatly reduce cell energy density because they are thick (~1mm) and dense (> 3g cm^{-3}). The SSE separator developed for this project's semi-solid Li/S cell design is pictured in Figure 1. It is a reinforced film of $(Li_2S)_{60}(SiS_2)_{28}(P_2S_5)_{12}$ (LiPSiS) glass SSE that is insoluble in DME:DOL based liquid electrolytes, largely impermeable to polysulfides, flexible, thin (~100 µm thick), light (< 2g cm^{-3}), and large enough for evaluation in a pouch cell format. To the author's knowledge, this project's semi-solid Li/S cell design is the first to utilize a sulfide SSE separator and the first to be demonstrated in a pouch cell format.

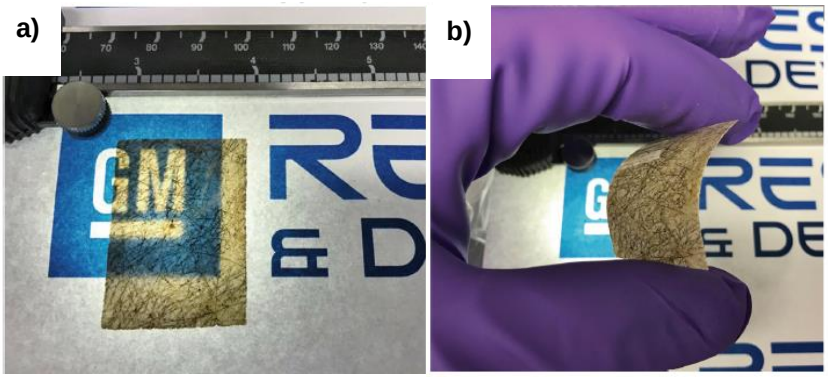

Figure 1. Pictures of reinforced LiPSiS glass SSE separators, which are translucent, bendable, and 135 – 180 µm thick. The dark brown crosshatch pattern is attributed to the underlying non-woven fiberglass reinforcement. Figures reproduced from [1].

Our cell designs utilizing a LiPSiS SSE separator are depicted in Figure 2. Cells were evaluated in both coin cell and single layer pouch cell formats. The conventional sulfur cathode had a nominal capacity of approximately 2.5 mAh cm^{-2}, the anode was 60 µm thick Li on stainless steel foil, and the liquid electrolyte was either 1:1 (v/v) DME:DOL + 1M LiTFSI or 1:1 (v/v) DME:DOL + 0.4M LiTFSI + 0.6M $LiNO_3$. More details are reported elsewhere [1].

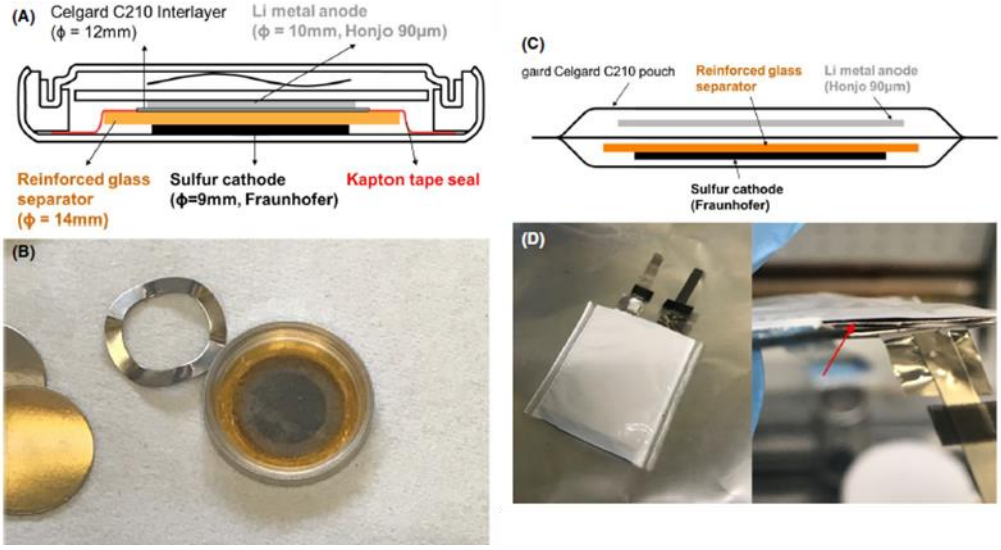

Figure 2. Schematics and pictures of the semi-solid Li/S cell designs developed for this project. a) Schematic of a semi-solid coin cell design. b) Top-down picture of a semi-solid coin cell with sulfur cathode sealed using an annular Kapton tape disc and a reinforced LiPSiS glass film separator. c) Schematic of a single layer semi-solid pouch cell design. The pouch cell casing is not included in the schematic. d) Top-down picture of a single layer semi-solid pouch cell core and a side-view picture of the same with the reinforced LiPSiS glass film separator indicated by a red arrow. Figures reproduced from [1].

Cycling data for this project's semi-solid Li/S cells are provided in Figure 3 and reported elsewhere [1]. In a first experiment utilizing the coin cell format (Figure 2a,b), a control cell and

a semi-solid cell were cycled with DME:DOL electrolyte containing no $LiNO_3$. The control cell (blue) never completed its first charge cycle due to the parasitic polysulfide shuttle. On the other hand, the semi-solid cell with LiPSiS SSE separator (red) quickly completed its first charge cycle and went on to cycle 300 cycles at a C/10 rate thereafter. An H-cell experiment with 0.1M Li_2S_4 solution confirmed that the LiPSiS separator acted as an impermeable barrier to polysulfides. Having shown that LiPSiS SSE separators block the polysulfide shuttle, a second experiment was conducted utilizing the single layer pouch cell format (Figure 2c,d). A LiPSiS SSE separator was shown to increase both cycle life and efficiency. We note that the semi-solid cell design presented here is a proof-of-concept and not fully optimized. Better design of the E/S and N/P ratios and the use of a thinner SSE separator are expected to improve cell cycle life and energy density to meet program targets.

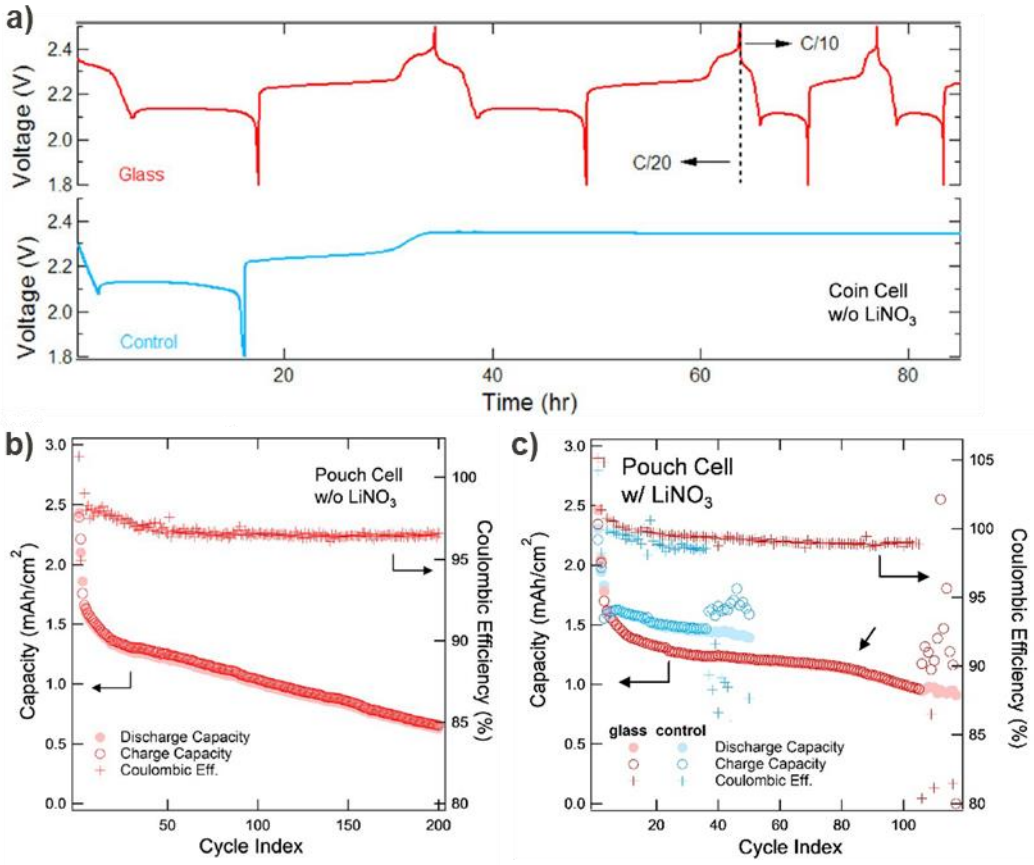

Figure 3. Cycling data for semi-solid Li/S coin and pouch cells with 1:1 (v/v) DME:DOL + 1M LiTFSI liquid electrolyte. a) Initial cycling behavior of coin cells without $LiNO_3$ co-salt. The semi-solid cell cycles normally while the control cell does not complete its first charge due to the parasitic polysulfide shuttle. b) Cycling data for a semi-solid pouch cell without $LiNO_3$ co-salt. c) Cycling data for control and semi-solid pouch cells with $LiNO_3$ co-salt. The LiPSiS SSE separator improves both cell cycle life and coulombic efficiency. Figures reproduced from [1].

The aforementioned semi-solid Li/S cell design was enabled by two technical achievements:

1) Fabrication of LiPSiS glass SSE separators and
2) Chemical compatibility of LiPSiS glass SSE with DME:DOL based liquid electrolyte.

In previous work, it was recognized that the moldability of glassy sulfide SSEs improved when consolidated at elevated temperature [14, 15]. Consolidation of glassy sulfide SSEs at elevated temperature will be referred to as hot pressing (HP). Similarly, consolidation of glassy SSEs at room temperature will be referred to as cold pressing (CP). The differential scanning calorimetry (DSC) scan for LiPSiS glass SSE is provided in Figure 4a and it shows two features; namely, a glass transition, T_g, at 322 °C and a crystallization onset, T_c, at 408 °C. When heated above the T_g, glasses enter a supercooled liquid state and viscosity drops dramatically [16]. This project utilized this effect to hot press tape cast films of LiPSiS glass SSE for 30 minutes at 330 °C and 12 MPa. The process is detailed in Figure 4 and elsewhere [1]. We note that a process temperature of only 330 °C is hundreds of degrees lower than that required to sinter oxide ceramic SSEs. A fiberglass non-woven paper was used to reinforce the brittle LiPSiS glass SSE. SEM images of the LiPSiS glass SSE film before and after hot pressing show that porosity was largely eliminated. In fact, the separator was over 93% dense and had an ionic conductivity of 0.7 mS cm^{-1} at room temperature.

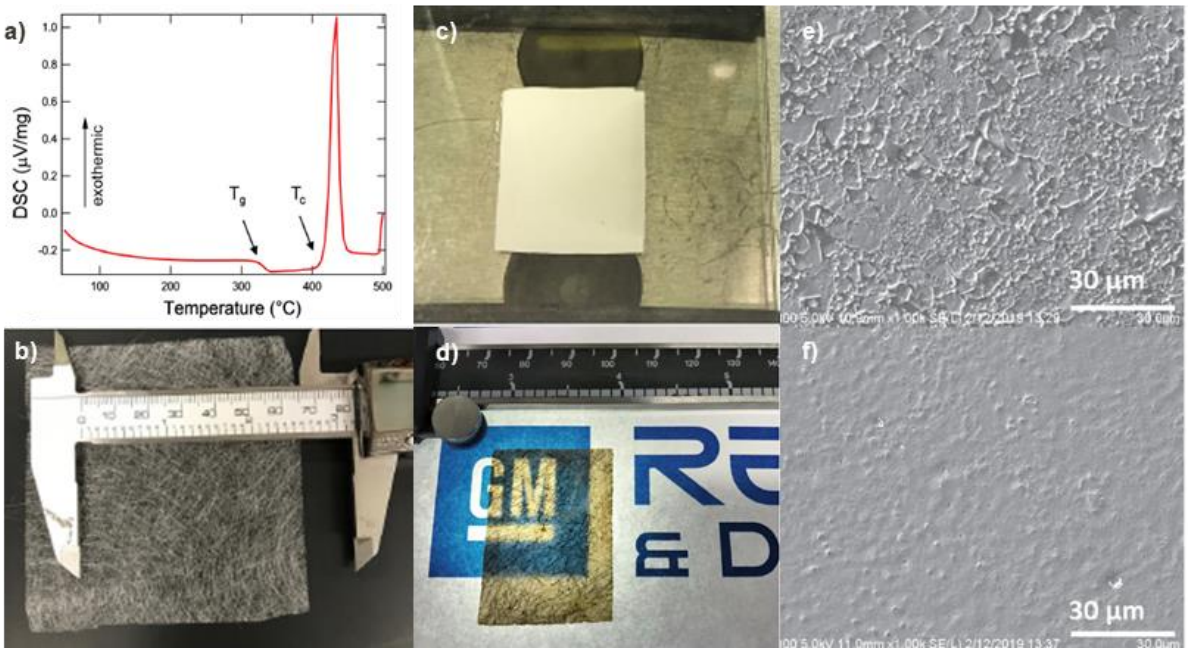

Figure 4. a) DSC scan for LiPSiS glass SSE with glass transition, T_g, and crystallization onset, T_c, indicated with arrows. b) A picture of the fiberglass non-woven (NW) paper used to reinforced the SSE separator. c) Picture of the green SSE/NW/SSE stack prior to hot pressing. d) Picture of the finished reinforced SSE separator after hot pressing. e) A SEM micrograph of a green SSE separator surface shows considerable porosity. f) A SEM micrograph of a hot-pressed SSE separator surface shows that the pores are largely eliminated. Figures reproduced from [1].

It is a generally held view that sulfide SSEs are not chemically compatible with ether-based solvents. In fact, there have been at least two reports of sulfide SSEs deposited from solutions composed of ether-based solvents [17, 18]. These SSE formulations, $(Li_2S)_{75}(P_2S_5)_{25}$ and

$Li_{10}GeP_2S_{12}$, were also found to be soluble in trigylme [19]. Therefore, it was non-obvious that LiPSiS glass SSE would be chemically compatible with a DME:DOL based liquid electrolyte (LE). To provide evidence of chemical compatibility, a series of $(Li_2S)_{60}(SiS_2)_x(P_2S_5)_{40-x}$ (x = 0, 4, 20, 28, 40) glass SSE compositions were soaked in 1:1 (v/v) DME:DOL and the results are provided in Figure 5 and reported elsewhere [2]. SiS_2-rich glass compositions x = 28 and 40 were insoluble in DME:DOL. This result was achieved because the Si-S bond (619 kJ mol^{-1}) is comparatively stronger than the P-S bond (346 kJ mol^{-1}). To demonstrate the utility of a semi-solid electrolyte system an experiment was conducted to determine the critical current densities (CCDs) of an all-solid-state Li/SSE/Li test cell and a semi-solid Li/LE/SSE/LE/Li test cell. As shown in Figure 6, the all-solid-state test cell required a stack pressure of 3 MPa to achieve a CCD of 1.8 mA cm^{-2}. The semi-solid test cell not only achieved a higher CCD of 3.0 mA cm^{-2}, but it did so at a stack pressure of only 0.1 MPa. This result is significant because it demonstrates how semi-solid cells have advantageous performance and operating specifications compared to all-solid-state cells.

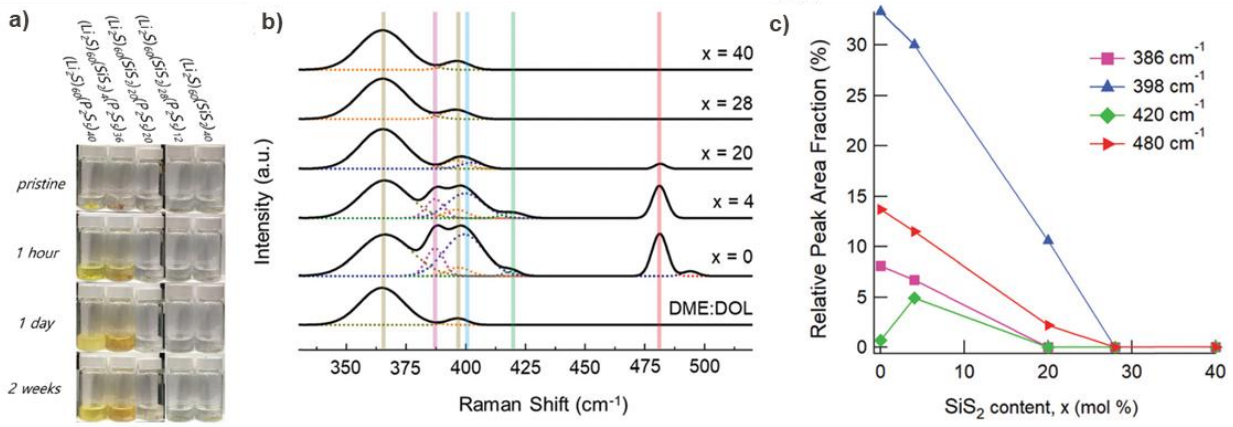

Figure 5. a) Solubility times series for $(Li_2S)_{60}(SiS_2)_x(P_2S_5)_{40-x}$ (x = 0, 4, 20, 28, 40) glasses soaked in DME:DOL. After 2 weeks the x = 0, 4 and 20 sample solutions showed signs of discoloration, which is attributed to dissolution of the glass. The x = 28 and 40 sample solutions remain clear over the course of the experiment. b) Raman spectra of pristine DOL:DME solvent and solutions obtained by soaking $(Li_2S)_{60}(SiS_2)_x(P_2S_5)_{40-x}$ (x = 0, 4, 20, 28, 40) glasses in DME:DOL. The location of structural unit vibrational modes are indicated with colored bars from left to right; namely, $P_2S_7^{4-}$ (pink), $P_2S_6^{4-}$ (blue), PS_4^{3-} (green), and S_8 (orange). Two vibrational modes of DME:DOL are also indicated (brown). c) Summary of dissolved species as a function of glass composition. Figures reproduced from [2].

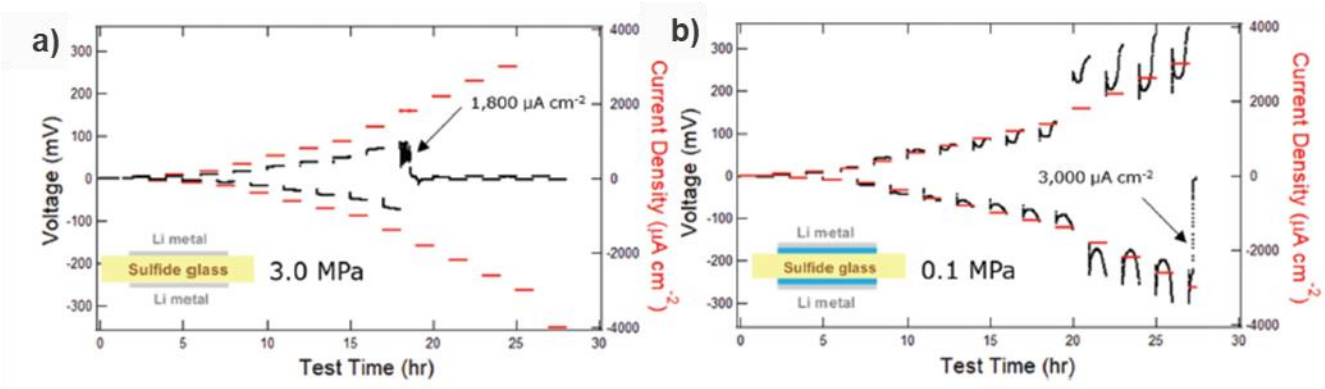

Figure 6. CCDs of symmetric Li/SSE/Li test cells with or without a liquid electrolyte interlayer and a different stack pressures at 25°C. The SSE separators are $(Li_2S)_{60}(SiS_2)_{28}(P_2S_5)_{12}$ glass wafers of approximately 600 µm thickness. a) An all-solid-state test cell with direct Li/SSE contact and 3 MPa stack pressure experiences shorting failure at a CCD of 1.8 mA cm^{-2}. b) A semi-solid test cell with liquid electrolyte Li/SSE interlayer and a 0.1 MPa stack pressure experiences shorting failure at a CCD of 3.0 mA cm^{-2}. Note: the test was paused for two days at 20 hours due to a planned facility power outage. Figures reproduced from [2].

II. Cell Design Opportunities

There are several opportunities to improve upon the cell design outlined in the first section and they will now be described to motivate the work described in the third section.

The primary benefit of an all-solid-state battery (ASSB) is improved abuse and thermal tolerance [20]. Unfortunately, a liquid or gel electrolyte used in a semi-solid battery design may reduce this tolerance somewhat. The first opportunity involves replacing the flammable and volatile DME:DOL based liquid electrolyte with a non-flammable alternative.

The second opportunity involves improving the moisture stability of sulfide SSEs. The semi-solid Li/S battery described in the first section was fabricated entirely inside an argon filled glovebox (<1 ppm H_2O), however, cell manufacturing typically takes place in dry rooms with a -40 °C dewpoint (127 ppm). To gauge the manufacturing readiness level of our cell technology, the stability of sulfide SSEs in a dry room environment must be evaluated and improved if necessary.

The third opportunity involves improving SSE separator design and there are several ways to do so. Glass thermal stability describes the tendency of a glass to devitrify (i.e. crystallize) once it is heated to a supercooled liquid state above its T_g. A glass that is thermal stability remains vitreous. The viscosity of a partially devitrified glass increases rapidly once the crystallites start to physically interact. Both LiPS and LiPSiS glasses have poor thermal stability and devitrify after hot pressing as shown in Figure 7 [1, 14]. As a result, a pressure of 12 MPa was required to consolidate the LiPSiS glass SSE separator to 93% density and 200 MPa to fully consolidate LiPS. Design of a thermally stable glass SSE composition would facilitate processing at lower pressures, which would allow the use of existing Li-ion battery calendaring equipment. The standalone LiPSiS glass SSE separator presented above also limits cell energy density because it is too thick.

To meet energy density targets it is required that the separator thickness be reduced to less than 40 µm [21]. To do so it is best to support the separator by the cathode. It follows that the cathode will also need to undergo the same hot pressing process required to consolidate the supported separator.

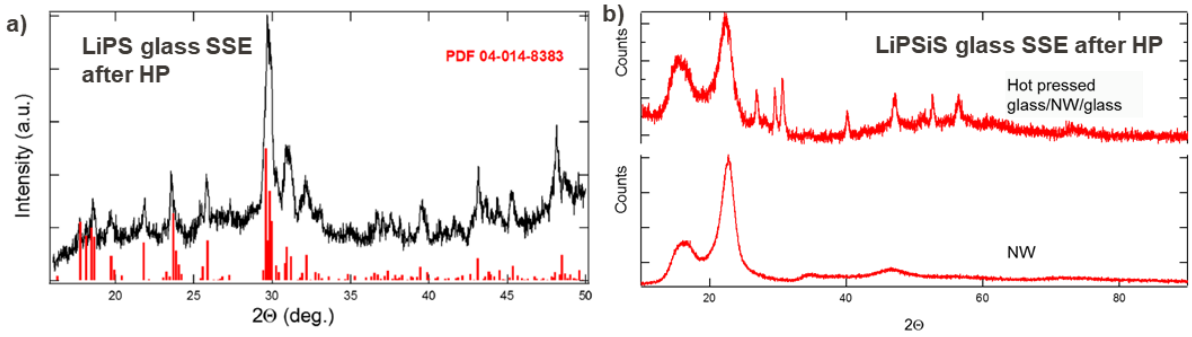

Figure 7. Both LiPS and LiPSiS glass SSEs exhibit poor thermal stability and devitrify when hot-pressed. Devitrification during hot pressing increases the viscosity of the glass in the supercooled liquid state. As a result, much higher pressures are required to consolidate the glasses. a) pXRD spectrum of LiPS glass SSE after hot pressing. b) pXRD spectrum of LiPSiS glass after hot pressing. Figures reproduced from [1, 14].

III. Progress Towards an Improved Cell Design

a. Moisture Stability Evaluated

The moisture stability of sulfide SSEs was systematically investigated as a function of SSE composition and dry room moisture setpoint [3]. A glovebox was retrofitted with a custom moisture control system as shown in Figure 8a,b to control water level to different moisture setpoints ranging from -76°C (<1 ppm H_2O) to -40°C (127 ppm H_2O) dewpoint. The setup consisted of an Arduino microcontroller, a moisture probe, and a cartridge-based desiccant system (VAC). A variety of different SSE compositions were studied; namely, $(Li_2S)_{75}(P_2S_5)_{25}$, $(Li_2S)_{70}(P_2S_5)_{30}$, $(Li_2O)_7(Li_2S)_{68}(P_2S_5)_{25}$, $(Li_2O)_7(Li_2S)_{63}(P_2S_5)_{30}$, and $(Li_2S)_{75}(P_2S_5)_{25}$ + 20 mol% LiI (LPSI). It was found that moisture stability improved with 75 mol% Li_2S modifier content and the introduction of a Li_2O co-modifier (Figure 8c,d). After a 30 min exposure in a −40°C dewpoint dry room environment the LPSI SSE powder generated 0.1 cc g^{-1} H_2S and its ionic conductivity decreased by over 50%. However, when the LSPI SSE powder was exposed as a slurry in an anhydrous dodecane carrier the same SSE generated 0 cc g^{-1} H_2S and its ionic conductivity only dropped by 14% (Figure 8e). Our results show that sulfide SSEs have acceptable moisture stability when appropriately processed in a dry room environment with anhydrous solvents and binders.

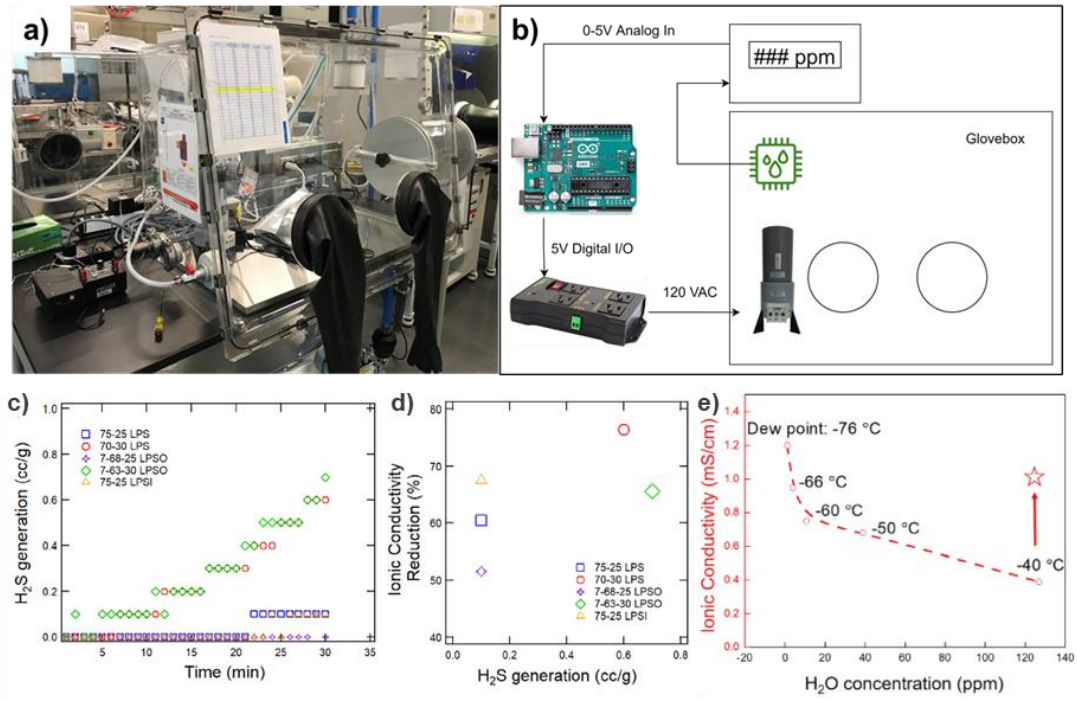

Figure 8. a) A picture of the experimental setup used to expose sulfide SSE powders to a dry room environment. The setup includes a 300L volume tabletop glovebox, a cartridge-based desiccant system, a microcontroller system to control the moisture setpoint, a personal H_2S detector, and a fan to continuously mix the glovebox air. b) Diagram of the experimental setup's control system to maintain moisture setpoints. c) H_2S generation of different SSEs in a −40°C dewpoint dry room

as a function of time. d) Reduction in ionic conductivity versus maximum H_2S reading for different sulfide SSEs. e) Ionic conductivity of LPSI sulfide SSE after exposure as a dry powder to different dry room environments for 30 min. The star marks the ionic conductivity of LPSI sulfide SSE after exposure to a −40°C dewpoint dry room for 30 min while immersed in anhydrous dodecane. Figures were reproduced from [3].

b. Oxysulfide SSE Processability

To improve the processability of glass SSE separators, it was desired to develop a more thermally stable SSE composition. As a reminder, thermal stability defines a glass' resistance to devitrification (i.e. crystallization). As shown in Figure 9a, $(Li_2S)_{70}(P_2S_5)_{30}$ sulfide glass SSE (LPS, 70:30) devitrifies extensively to the $Li_7P_3S_{11}$ ceramic phase after hot pressing. As mentioned earlier, this results in the need for a high processing pressure (200 MPa) to fully consolidate the material because devitrified glasses are highly viscous. Oxygen can be added to $(Li_2S)_{70}(P_2S_5)_{30}$ glasses by including a P_2O_5 co-former. When 5 mol% P_2O_5 is added, it was found that $(Li_2S)_{70}(P_2S_5)_{25}(P_2O_5)_5$ oxysulfide glass SSE (LPSO, 70:25:5) remained largely vitreous after hot pressing (Figure 9b). In fact, when hot-pressed at 230°C, LPSO, 70:25:5 had a devitrification rate that was 10 times slower than that of LPS, 70:30 (Figure 9c). Oxygen atoms in LPSO, 70:25:5 are accommodated into a $Li_7P_3S_{9.75}O_{1.25}$ ceramic phase that is isostructural with the $Li_7P_3S_{11}$ ceramic phase [22]. The devitrification rate of LPSO, 70:25:5 is slower because the smaller radius of the O^{2-} anion (140 pm) compared to the S^{2-} anion (184 pm) sterically hinders atomic rearrangement during the crystallization process (Inset Figure 9c).

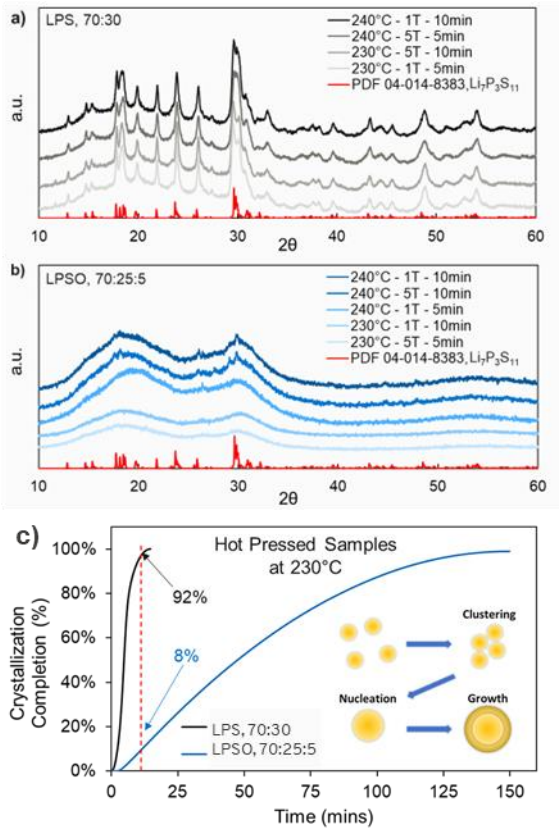

Figure 9. a) pXRD of LPS, 70:30 samples after hot-pressing using various protocols. b) pXRD of LPSO, 70:25:5 samples after hot-pressing using various protocols c) DSC crystallization completion of LPS, 70:30 vs. LPSO, 70:25:5 at 230°C. Bottom right inset graphic illustrates the crystallization process of crystallite nucleation and growth. The poor thermal stability of the LiPS glass leads to extensive devitrification, whereas the thermally stable LiPSO glass remains largely vitreous.

Having established that the LPSO, 70:25:5 oxysulfide glass SSE is thermally stable, a series of hot pressing trials were conducted using a variety of different processing conditions (Figure 10a). In each case, the oxysulfide SSE was more deformable than the sulfide SSE. Informed by the optimal process condition, a 40 cm^2 separator film of LPSO, 70:25:5 oxysulfide glass SSE was prepared by hot pressing at a temperature of 230 ºC and a pressure of only 2.75 MPa. The film was 110 µm thick, 91.4% dense, and had an ionic conductivity of 0.75 mS/cm after annealing. We conclude that the LPSO, 70:25:5 oxysulfide glass SSE is highly processable and sought to apply it next as a catholyte in all-solid-state cathodes.

Figure 10. a) Picture of LPS, 70:30 and LPSO, 70:25:5 reinforced pellets after hot pressing using various protocols. In general, the LPSO, 70:25:5 samples are much more deformable than the LPS, 70:30 samples. b) Picture of a hot-pressed standalone, reinforced LPSO, 70:25:5 SSE separator film. The film is flexible and translucent. c) Close up picture of the same film after being cut into a disc. The crosshatch pattern is attributed to the underlying non-woven fiber reinforcement.

c. Hot-Pressed Cathode Composites

All-solid-state cathodes are advantageous for two reasons. First, the utilization of a SSE catholyte improves SSB abuse and thermal tolerance because it displaces liquid electrolyte, which may be volatile and flammable. Second, an all-solid-state cathode is better suited at supporting a SSE separator. As mentioned in the second section, cathode-support provides a means to

reduce the thickness of SSE separators to an extent that cell energy targets are met. It follows that the cathode support must also undergo the same hot pressing process as the supported separator. Therefore, the goal of this work was to show that hot pressing can also improve the performance of all-solid-state electrodes by increasing the solid-solid interface between active material (AM) and SSE. In the first phase of work, we investigated the hot pressing of NCM cathode composites. In the second phase of work, we investigated the hot pressing of low voltage AM cathode composites.

The effectiveness of hot pressing NCM cathode composites was explored by systematically evaluating combinations of NCM622 and NCM85105 AMs with glassy Li_3PS_4, glassy $Li_7P_3S_{11}$, and β-Li_3PS_4 SSEs [4]. As shown in Figure 11, the performance of a NCM622 + β-Li_3PS_4 composite cathode was improved by hot-pressing at 200 °C and 370 MPa for 10 minutes. While the hot-pressed (HP) cathode initially delivered a lower specific capacity (Figure 11a), its capacity retention at a C/10 rate was much improved compared to a cold-pressed (CP) control cell (Figure 11b). It was found that NCM reacted with certain SSE compositions, producing insulating interfacial decomposition products that increased cell impedance and reduced specific capacity (Figure 12a). Unfortunately, the SSE that was the most stable versus NCM (i.e. β-Li_3PS_4), was also the least moldable SSE. As shown in Table 1, the cathode composite with β-Li_3PS_4 was still 26.7% porous after hot-pressing. It is advantageous to reduce cathode composite porosity as much as possible because it increases cell energy density. In addition, secondary NCM particles were susceptible to cracking at the pressures required to consolidate β-Li_3PS_4 (Figure 12b,c). In conclusion, it was desired to replace high voltage NCM AM with a stable and mechanically robust low voltage AM so that the most moldable SSE catholyte could be utilized.

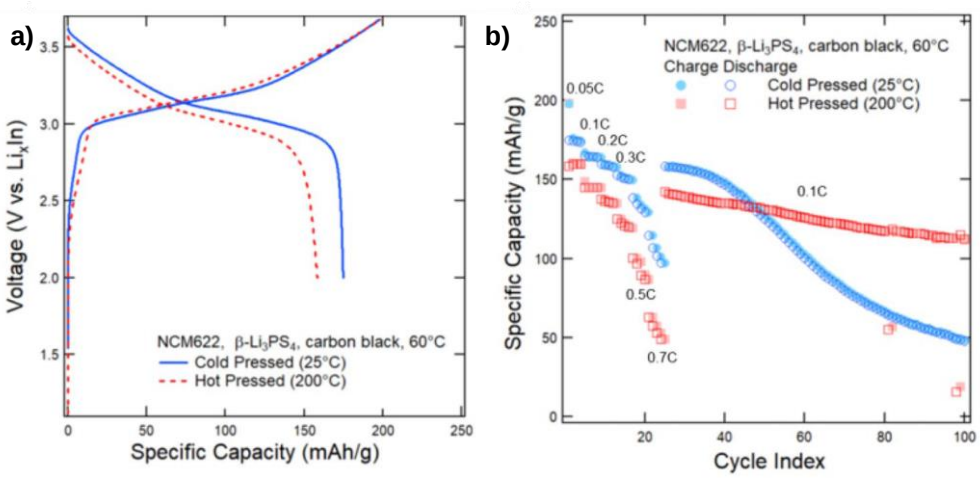

Figure 11. a) First cycle voltage profiles for cold-pressed (blue) and hot-pressed (red) cathode composites with NCM622 active material, β-Li_3PS_4 SSE, and carbon black conductive additive. b) Cyclic capacities for the same. Though the hot-pressed cell initially delivers lower capacity, it goes on to retain its capacity better than the cold-pressed cell. Figures reproduced from [4].

Table 1. Densities and porosities of cold-pressed and hot-pressed NCM cathode composites.

Material system	CP density (g/cc)	HP density (g/cc)	CP porosity (%)	HP porosity (%)
glassy Li_3PS_4 + NCM85105	2.95	3.19	13.5	6.5
glassy Li_3PS_4 + NCM622	2.863	3.149	17.1	8.86
β-Li_3PS_4 + NCM85105	2.36	2.47	29.7	26.7
glassy $Li_7P_3S_{11}$ + NCM622	2.863	3.499	17.8	0

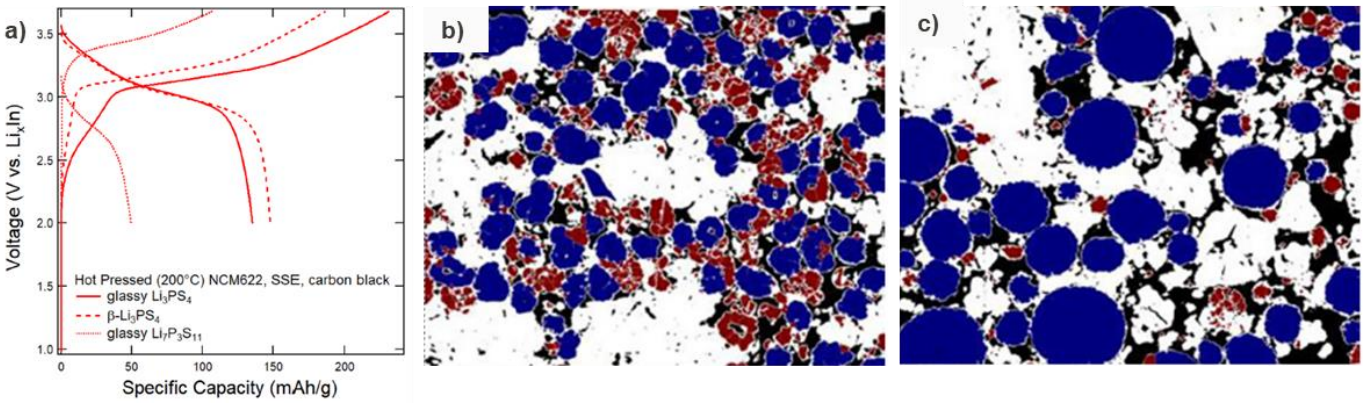

Figure 12. a) First cycle voltage profiles for NCM622 composites with either glassy Li_3PS_4 (solid), β-Li_3PS_4 (dash), or glassy $Li_7P_3S_{11}$ (dot) SSEs and 2 wt.% carbon black additive. b) Processed SEM image of a hot-pressed NCM85105/βLi_3PS_4 cathode composite. c) Processed SEM image of a hot-pressed NCM622/β-Li_3PS_4 cathode composite. The color scheme for the processed images is as follows: white = SSE particle, black = pore, blue = intact NCM particle, and red = damaged NCM particle. Figures reproduced from [4].

In the second phase of the all-solid-state cathode work, NCM was replaced with a low voltage AM. Furthermore, highly processable LPSO oxysulfide glass SSE was used as the catholyte. Hot pressing at 240 °C and 47 MPa for 10 minutes reduced the porosity of low voltage AM + LPSO cathode composites from ~30% to ~20% (Figure 13). DSC scans of NCM and low voltage AM cathode composites are provided in Figure 13d. The NCM cathode composites reveal large exothermic signals that are attributed to an interfacial reaction between the NCM and the sulfide SSE. On the other hand, the low voltage AM cathode composites exhibit no exothermic signals related to interfacial decomposition. Small exothermic signals at approximately 250 °C are attributed to devitrification of the LPSO glass SSE. The electrochemical performance of CP and HP cells with low voltage AM + LPSO cathode composites are provided in Table 2. When cycled at 25 °C, a CP cell delivered negligible capacity whereas a HP cell delivered a 1st cycle discharge capacity in excess of 600 mAh g^{-1}. Furthermore, the cell impedance was reduced from 4010 Ω to 127 Ω by hot pressing. When cycled at 60°C, the HP cell also shows improved performance up to

50 cycles (Figure 14). Improved HP cell performance is attributed to better AM/SSE interfacial contact and the absence of insulating interfacial decomposition products. This result was achieved by selecting mechanically robust and stable low voltage AM and highly processable LPSO glass SSE catholyte. In conclusion, we demonstrated a viable cathode support for hot-pressed SSE separators.

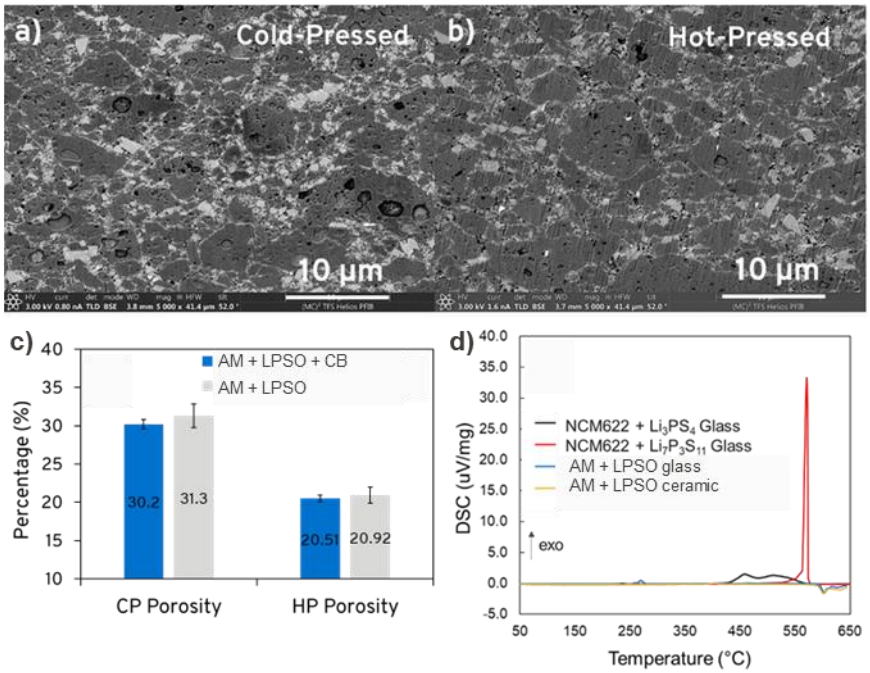

Figure 13. SEM images of cathode composite composed of a low voltage active material (AM) and LPSO glass SSE a) before and b) after hot pressing. c) Porosity of cathode composites before and after hot pressing. d) DSC scans of NCM622 and low voltage AM cathode composites. The NCM622 cathode composites exhibit large exothermic reactions indicative a reaction between the NCM622 and the LPS SSE. On the other hand, the low voltage AM cathode composite exhibit no exothermic reactions in the same temperature range. Small exothermic signals around 250°C are attributed to the devitrification of the glassy SSEs.

Table 2. Summary of electrochemical characterization of cells with cathode composites composed of low voltage active material (AM) and highly processable LPSO glassy SSE.

Press	Temperature (°C)	Spec. Cap. @ C/20 (mAh g^{-1})	EIS (Ω)
CP	25	0	4010
CP	60	588.9	150
HP	25	657.8	127
HP	60	801.3	47

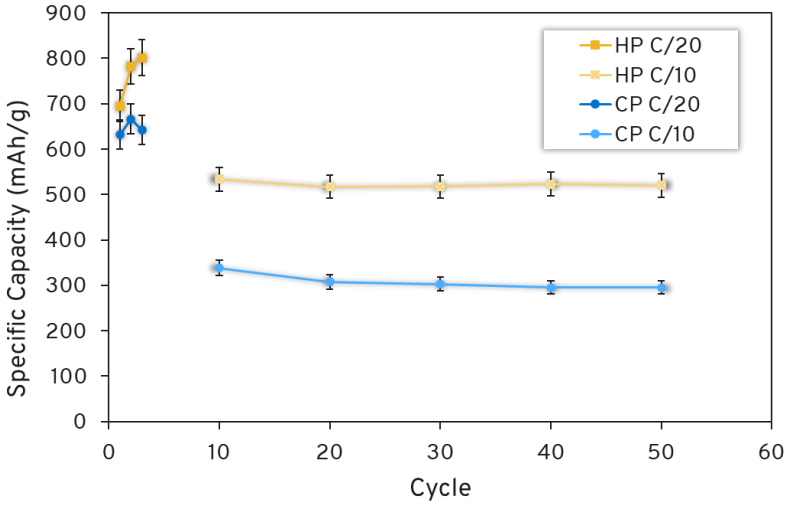

Figure 14. Cyclic capacity of cells with cathode composites composed of low voltage active material (AM) and highly processable LPSO glassy SSE cycled at 60°C. Hot pressing (HP) improves the utilization of AM by nearly 70% compared to cold pressing (CP).

d. Semi-Solid Electrolyte

The final avenue explored to improve upon our semi-solid Li/S cell design involved replacing the DME:DOL based liquid electrolyte with a solvate ionic liquid (SIL) electrolyte. As shown in Figure 15, SIL electrolyte is less flammable than DME:DOL based liquid electrolyte, which will improve future cell abuse and thermal tolerance. As before, chemical compatibility between the SSE and the LE is of the utmost importance. Fortunately, it was previously reported that $Li_{10}GeP_2S_{12}$ is stable in SIL [19], however, SIL are often highly viscous and cause poor reaction kinetics. Consequently, it may be desirable to utilize dilute SIL for improved wettability and enhanced reaction kinetics. In Figure 16 we show that oxysulfide SSE are more stable in dilute SIL than sulfide SSE. A variety of (oxy)sulfide glass SSE samples were soaked in SIL for 7 days. It was found that sample mass loss decreased with increasing oxygen content (Figure 16b). SILs were

also characterized with UV-Vis spectroscopy after 7 days and reduced absorbance was associated increased oxygen content. We conclude that a combination of oxysulfide SSE and SIL provides a promising semi-solid electrolyte system for future semi-solid battery designs.

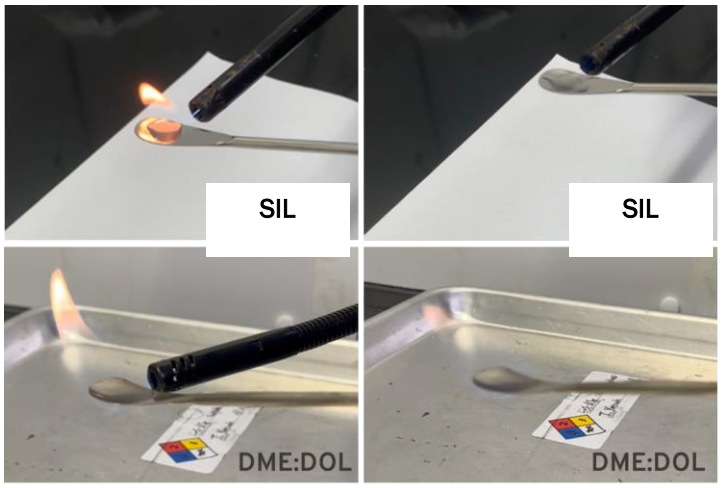

Figure 15. Pictures of a solvate ionic liquid (SIL) electrolyte and a DME:DOL + 1M LiTFSI electrolyte under an exposed flame. The DME:DOL electrolyte readily ignites whereas the SIL does not.

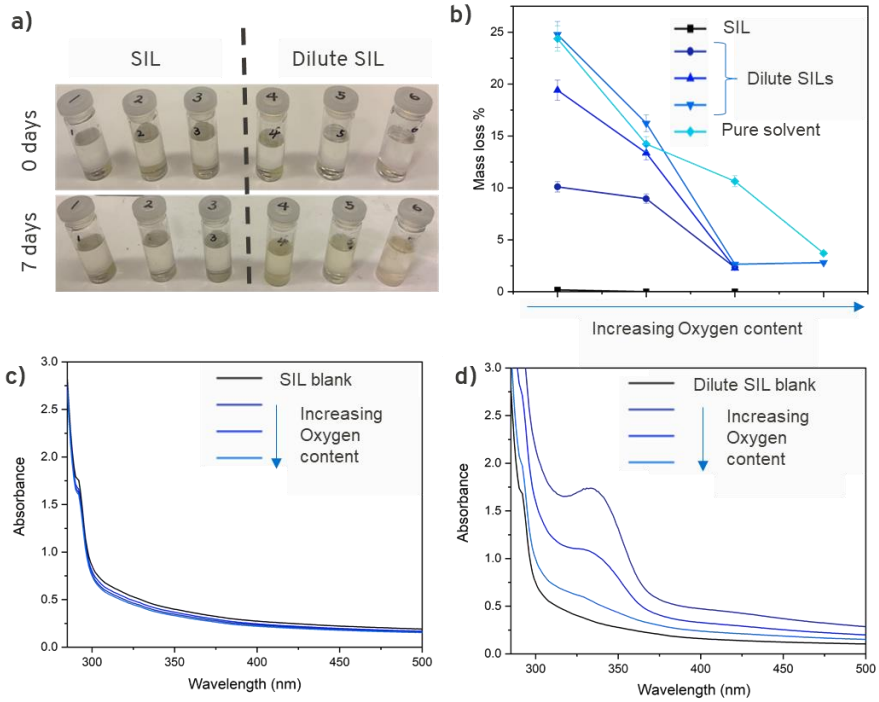

Figure 16. a) Picture of (oxy)sulfide glass SSE samples soaked in SIL and dilute SIL. b) Mass loss of (oxy)sulfide glass SSE samples after soaking in a variety of SIL for 7 days. Reduced mass loss is associated with increased SSE oxygen content. c) UV-Vis spectra of (oxy)sulfide SSE samples after

soaking in SIL for 7 days. d) UV-Vis spectra for (oxy)sulfide SSE samples after soaking in dilute SIL for 7 days. Reduced absorbance is associated with increased SSE oxygen content.

Conclusions

High profile research on solid-state electrolytes typically focuses on alluring attributes like high ionic conductivity and the discovery of new ceramic phases. In this project, we focused on the often neglected attributes of processability (i.e. crystallization kinetics), chemical stability, and moisture stability. As a result, we were rewarded with the demonstration of a semi-solid Li/S cell design capable of meeting program targets.

Key Publications

Peer Reviewed Journal Articles

1) Yersak, Thomas, James R. Salvador, Robert D. Schmidt, and Mei Cai. "Hybrid Li-S pouch cell with a reinforced sulfide glass solid-state electrolyte film separator." *International Journal of Applied Glass Science* 12.1 (2021): 124-134.
2) Albertus, Paul, et al. "Challenges for and pathways toward Li-metal-based all-solid-state batteries." *ACS Energy Letters* 6.4 (2021): 1399-1404.
3) Yersak, Thomas A., Fang Hao, Chansoon Kang, James R. Salvador, Qinglin Zhang, Hernando Jesus Gonzalez Malabet, and Mei Cai. "Consolidation of composite cathodes with NCM and sulfide solid-state electrolytes by hot pressing for all-solid-state Li metal batteries." *Journal of Solid State Electrochemistry* 26.3 (2022): 709-718.
4) Yersak, Thomas A., Chansoon Kang, James R. Salvador, Nicholas PW Pieczonka, and Mei Cai. "Sulfide glass solid-state electrolyte separators for Li metal batteries: using an interlayer to increase rate performance and reduce stack pressure." *Materials Advances* 3.8 (2022): 3562-3570.
5) Yersak, Thomas A., Yubin Zhang, Fang Hao, and Mei Cai. "Moisture Stability of Sulfide Solid-State Electrolytes." *Frontiers in Energy Research* 10:882508 (2022).

Invited Seminars

6) Yersak, Thomas. “Solid-State Electrolyte Separator Development at GM R&D.” Iowa State University, 27 September 2021. Invited seminar.
7) Yersak, Thomas. “Process Rheology of Oxysulfide Solid-State Electrolyte Separators for Solid-State Batteries.” ACS (American Chemical Society) Fall Meeting, 22 August 2022. Invited seminar.
8) Yersak, Thomas. “Sulfide Glass Solid-State Electrolyte Separators for Li Metal Batteries: Using an Interlayer to Increase Rate Performance and Reduce Stack Pressure.” TechBlick Solid-State Batteries: Innovations, Promising Start-ups, & Future Roadmap, 16 February 2023. Invited seminar.
9) Yersak, Thomas. “Moisture Stability of Sulfide Solid-State Electrolytes.” MRS (Material Research Society) Spring Meeting, 25 April 2023. Invited seminar.

10) Yersak, Thomas. “Sulfide Glass Solid-State Electrolyte Separators for Li Metal Batteries: Using an Interlayer to Increase Rate Performance and Reduce Stack Pressure.” BEV (Battery & Electric Vehicles) Conference, 3 May 2023. Invited seminar.

Patent Applications

11) Gonzalez Malabet, Hernando Jesus, Thomas Yersak, and Yubin Zhang. “Solid-State Electrolyte Materials for All-Solid-State Batteries.” US Application 17/824,584.
12) Zhang, Yubin, Thomas Yersak, and Ion Halalay. “Bicontinuous Separating Layers for Solid-State Batteries and Methods of Forming the Same.” US Application 17/955,151.
13) Gonzalez Malabet, Hernando Jesus, Thomas Yersak, and Aaron Ketchum. “Removable Binder for Hot-Pressed Solid-State Electrolyte Separators.” US Application 18/080,864.
14) Zhang, Yubin, Thomas Yersak, and Aaron Ketchum. “Semi-Solid State Electrolyte System Including an Oxysulfide Solid-State Electrolyte and Solvate Ionic Liquid” US Application 18/169,686

References

1. Yersak, T., et al., *Hybrid Li-S pouch cell with a reinforced sulfide glass solid-state electrolyte film separator.* International Journal of Applied Glass Science, 2021. **12**(1): p. 124-134.
2. Yersak, T.A., et al., *Sulfide glass solid-state electrolyte separators for Li metal batteries: using an interlayer to increase rate performance and reduce stack pressure.* Materials Advances, 2022. **3**(8): p. 3562-3570.
3. Yersak, T.A., et al., *Moisture Stability of Sulfide Solid-State Electrolytes.* Frontiers in Energy Research, 2022. **10**: p. 882508.
4. Yersak, T.A., et al., *Consolidation of composite cathodes with NCM and sulfide solid-state electrolytes by hot pressing for all-solid-state Li metal batteries.* Journal of Solid State Electrochemistry, 2022. **26**(3): p. 709-718.
5. Ye, H. and Y. Li, *Towards practical lean-electrolyte Li–S batteries: Highly solvating electrolytes or sparingly solvating electrolytes?* Nano Research Energy, 2022. **1**(1): p. e9120012.
6. Jozwiuk, A., et al., *The critical role of lithium nitrate in the gas evolution of lithium–sulfur batteries.* Energy & Environmental Science, 2016. **9**(8): p. 2603-2608.
7. Zhang, S.S., *Role of LiNO3 in rechargeable lithium/sulfur battery.* Electrochimica Acta, 2012. **70**: p. 344-348.
8. Wang, L., Y. Wang, and Y. Xia, *A high performance lithium-ion sulfur battery based on a Li 2 S cathode using a dual-phase electrolyte.* Energy & Environmental Science, 2015. **8**(5): p. 1551-1558.
9. Yu, X., et al., *Hybrid lithium–sulfur batteries with a solid electrolyte membrane and lithium polysulfide catholyte.* ACS applied materials & interfaces, 2015. **7**(30): p. 16625-16631.
10. Zhou, W., et al., *Plating a dendrite-free lithium anode with a polymer/ceramic/polymer sandwich electrolyte.* Journal of the American Chemical Society, 2016. **138**(30): p. 9385-9388.

11. Yu, X., et al., *Polysulfide-shuttle control in lithium-sulfur batteries with a chemically/electrochemically compatible NASICON-type solid electrolyte.* Advanced Energy Materials, 2016. **6**(24): p. 1601392.
12. Wang, Q., et al., *A gel-ceramic multi-layer electrolyte for long-life lithium sulfur batteries.* Chemical communications, 2016. **52**(8): p. 1637-1640.
13. Li, Y., et al., *Hybrid polymer/garnet electrolyte with a small interfacial resistance for lithium-ion batteries.* Angewandte Chemie International Edition, 2017. **56**(3): p. 753-756.
14. Yersak, T., et al., *Hot pressed, fiber-reinforced (Li2S) 70 (P2S5) 30 solid-state electrolyte separators for Li metal batteries.* ACS Applied Energy Materials, 2019. **2**(5): p. 3523-3531.
15. Garcia-Mendez, R., et al., *Correlating macro and atomic structure with elastic properties and ionic transport of glassy Li2S-P2S5 (LPS) solid electrolyte for solid-state Li metal batteries.* Advanced Energy Materials, 2020. **10**(19): p. 2000335.
16. Shelby, J.E., *Introduction to glass science and technology*. 2020: Royal society of chemistry.
17. Lim, H.D., et al., *Solid electrolyte layers by solution deposition.* Advanced Materials Interfaces, 2018. **5**(8): p. 1701328.
18. Xiao, Q., et al., *Electrolyte and Electrode Structure*. 2016, GM Global Technology Operations LLC.
19. Oh, D.Y., et al., *Excellent compatibility of solvate ionic liquids with sulfide solid electrolytes: toward favorable ionic contacts in bulk-type all-solid-state lithium-ion batteries.* Advanced Energy Materials, 2015. **5**(22): p. 1500865.
20. Inoue, T. and K. Mukai, *Are all-solid-state lithium-ion batteries really safe?–verification by differential scanning calorimetry with an all-inclusive microcell.* ACS Applied Materials & Interfaces, 2017. **9**(2): p. 1507-1515.
21. Berg, E.J. and S. Trabesinger, *Viability of polysulfide-retaining barriers in Li–S battery.* Journal of The Electrochemical Society, 2017. **165**(1): p. A5001.
22. Minami, K., et al., *Structure and properties of the 70Li2S·(30− x) P2S5· xP2O5 oxysulfide glasses and glass–ceramics.* Journal of non-crystalline solids, 2008. **354**(2-9): p. 370-373.

Acknowledgements

The PI (Thomas A. Yersak) would like to recognize our NETL managers, Adrienne L Riggi and Coriana H. Fitz, and our GM Government Contracts Manager, Aida Rodrigues. Special thanks is also given to Drs. James R. Salvador, Yubin Zhang, Hernando Jesus Gonzalez Malabet, Fang Hao, and Chansoon Kang for their important contributions to the project.

This material is based upon work supported by the U.S. Department of Energy's Office of Energy Efficiency and Renewable Energy (EERE) under the Award Number DE-EE0008857. This report was prepared as an account of work sponsored by an agency of the United States Government. Neither the United States Government nor any agency thereof, nor any of their employees, makes any warranty, express or implied, or assumes any legal liability or responsibility for the accuracy, completeness, or usefulness of any information, apparatus, product, or process disclosed, or represents that its use would not infringe privately owned rights. Reference herein

to any specific commercial product, process, or service by trade name, trademark, manufacturer, or otherwise does not necessarily constitute or imply its endorsement, recommendation, or favoring by the United States Government or any agency thereof. The views and opinions of authors expressed herein do not necessarily state or reflect those of the United States Government or any agency thereof.